Histologic Spectrum of Giant Cell Tumor (GCT) of Bone in Patients 18 Years of Age and Below

A Study of 63 Patients

Alyaa Al-Ibraheemi, MD, Carrie Y. Inwards, MD,* Riyam T. Zreik, MD,* Doris E. Wenger, MD,† Sarah M. Jenkins, MS,‡ Jodi M. Carter, MD, PhD,* Jennifer M. Boland, MD,* Peter S. Rose, MD,§ Long Jin, MD,* Andre M. Oliveira, MD, PhD,* and Karen J. Fritchie, MD**

Abstract: Although the majority of giant cell tumors (GCTs) of the bone occur in adult patients, occasionally they arise in the pediatric population. In this setting they may be mistaken for tumors more commonly seen in this age group, including osteosarcoma, aneurysmal bone cyst, and chondroblastoma. All cases of primary GCT of the bone arising in patients 18 years and below were retrieved from our institutional archives and examined with emphasis on the evaluation of various morphologic patterns. Clinical/radiologic records were reviewed when available. Analysis for *H3F3A*/*H3F3B* mutations was performed in a subset of cases. Sixty-three (of 710) patients treated at our institution for GCT were 18 years of age and below. The following morphologic patterns were identified: fibrosis (31 cases, 49%), reactive-appearing bone (26, 41%), cystic change (7, 11%), foamy histiocytes (6, 10%), secondary aneurysmal bone cyst (3, 5%), and cartilage (2, 3%). Infarct-like necrosis was present in 17 tumors (27%), and the mitotic rate ranged from 0 to 35 mitoses/10 high-power fields (median 5 mitoses/10 high-power field). Follow-up information (n = 55; 6 mo to 69.6 y; median, 11.6 y) showed 21 patients with local recurrence (38%) and 2 patients with lung metastasis (4%). Polymerase chain reaction with sequencing showed that 5 of 5 tested cases harbored *H3F3A* mutations. In summary, GCT arising in the pediatric population is rare, representing 9% of GCTs seen at our institution. The morphologic spectrum of these tumors is broad and similar to that seen in patients above 18 years of age. It is important to recognize that matrix formation may be observed in GCT, including reactive-appearing bone and cartilage, as well as areas of fibrosis mimicking osteoid production, to avoid misclassification as osteosarcoma or other giant cell–rich lesions common in children.

From the Departments of *Laboratory Medicine and Pathology; †Radiology; ‡Biomedical Statistics and Informatics; and §Orthopedic Surgery, Mayo Clinic, Rochester, MN.

Conflicts of Interest and Source of Funding: The authors have disclosed that they have no significant relationships with, or financial interest in, any commercial companies pertaining to this article.

Correspondence: Karen J. Fritchie, MD, Department of Anatomic Pathology, Mayo Clinic, Hilton 11, 200 First Street, SW, Rochester, MN 55905 (e-mail: Fritchie.Karen@Mayo.edu).

Key Words: giant cell tumor of bone, pediatric, osteosarcoma, aneurysmal bone cyst

(*Am J Surg Pathol* 2016;40:1702–1712)

Giant cell tumor (GCT) of the bone represents 4% to 5% of all primary bone tumors and most commonly involves the distal femur, proximal tibia, and distal radius.[1–3] GCT, along with chondroblastoma and clear cell chondrosarcoma, forms a classic triad of bone neoplasms that involve the epiphysis, with GCT and clear cell chondrosarcoma usually occurring in skeletally mature patients.[2–5] The diagnosis of GCT is relatively straightforward in cases with classic morphology, including bland-appearing mononuclear cells in a background of uniformly distributed giant cells, occurring in an epiphyseal location in patients older than 18 years. However, diagnostic challenges may arise in the pediatric age group when the lesion contains nonclassic histologic features or spares the epiphysis. Specifically, GCT in pediatric patients may raise concern for osteosarcoma if the lesion contains bone, has conspicuous mitoses, or predominantly involves the metaphysis. Furthermore, other giant cell–rich lesions that commonly occur in this age group such as aneurysmal bone cyst and chondroblastoma may also enter the differential diagnosis.

Although GCT in the pediatric age group has been described,[2–19] these reports focus on the radiologic features of these tumors in the pediatric population or combine the histologic findings of pediatric and adult cases. We studied a large series of GCTs in patients 18 years of age and younger with an emphasis on morphologic patterns identified in the tumors of this population. As recent work has found that *H3F3A*/*H3F3B* mutations are potentially useful for the diagnosis of GCT and chondroblastoma, respectively, we analyzed a subset of cases for these mutations.[20–23]

MATERIALS AND METHODS

This study was approved by the Institutional Review Board at Mayo Clinic. All curettage and resection specimens of primary "giant cell tumor of bone" from

patients 18 years old or younger were retrieved from our institutional archives. Recurrent and metastatic tumors were excluded, as were cases of malignant GCT. All available hematoxylin and eosin slides were reviewed by experienced bone pathologists (K.J.F., J.M.C., J.M.B., and C.Y.I.) to confirm the diagnosis. The cataloged morphologic patterns included reactive-bone formation, hyaline cartilage, fibrosis, foamy macrophages, cystic change, and secondary aneurysmal bone cyst formation. Fibrosis was morphologically subclassified into the following patterns: loose, pericellular, hyalinized, geographic, septal, and lace-like. The presence of infarct-like necrosis and cytologic atypia was also assessed. Mitotic rates in the area of highest mitotic activity were recorded per 10 high-power fields (HPF).

Available radiologic images were reviewed by a musculoskeletal radiologist (D.E.W.) with attention to location, radiologic features, extent of involvement, skeletal maturity, and associated pathologic fracture. For cases without available imaging, we retrieved previously recorded radiologic reports from the patient's medical record. Clinical information including age, sex, and follow-up data was obtained from medical records.

Five cases of GCT were tested for *H3F3A and H3F3B* mutations by polymerase chain reaction (PCR) and Sanger sequencing. Genomic DNA was extracted from FFPE tissues using the phenol/chloroform method. The PCR primers used in this study are as follows: 5′-AAATCGACCGGTGGTAAAGC (forward) and 5′-ATACAAGAGAGACTTTGTCCCA (reverse) for *H3F3A*; 5′-GTAAGTCCACCGGTGGGAAA (forward) and 5′-AGGAGTGAGCGGACGCTGCC (reverse) for *H3F3B*. After PCR amplification, PCR products of *H3F3A* (145 bp) and *H3F3B* (170 bp) underwent Sanger sequencing to detect the mutation hotspots of *H3F3A* (exon 2, code 34) and *H3F3B* (exon 2, code 36).

Patient and tumor characteristics were summarized with frequencies and percentages or with medians and ranges, as appropriate. Features were compared between categories with the Fisher exact tests for categorical data and with Wilcoxon rank-sum tests for continuous data. Progression-free survival was summarized at 5 years with

FIGURE 1. Anteroposterior (A) and lateral radiographs (A) demonstrate an osteolytic lesion in the proximal radial metadiaphysis in a 17-year-old girl with GCT. The lesion is associated with mild expansion of the bone and a subtle nondisplaced pathologic fracture (arrow in B). The lesion extends to the growth plate but spares the epiphysis. Sagittal T1 (C), fat-suppressed T2 (D), and gadolinium-enhanced spoiled gradient echo (E), magnetic resonance images show a mixed solid and cystic lesion in the proximal radial metadiaphysis with sparing of the proximal epiphysis (arrow in C). The lesion demonstrates a heterogenous signal with evidence of low T2 signal solid enhancing tissue proximally (rectangle) and a cystic, minimally enhancing component distally (circle). There is periosteal reaction and edema in the surrounding soft tissues related to the nondisplaced pathologic fracture.

TABLE 1. Radiologic Data for Bones With Epiphysis or Epiphyseal Equivalent (N = 33)

Extend of Involvement	n (%)	M/F	Age Range (y)	Median Age (y)
Epiphysis only	3 (9)	2/1	13-18	18
Metaphysis and epiphysis	23 (70)	5/18	8-18	17
Metaphysis with extensive epiphyseal involvement	18	4/14	15-18	17
Metaphysis with minimal epiphyseal involvement	5	1/4	8-18	16
Metaphysis without epiphysis	7 (21)	3/4	9-16	13

F indicates female; M, male.

the Kaplan-Meier method (including 95% confidence intervals) and was compared with patient and tumor characteristics with Cox proportional hazards regression using likelihood ratio tests. All analyses were performed using SAS version 9.4 (SAS Institute Inc., Cary, NC) and R.[24] *P*-values <0.05 were considered statistically significant.

RESULTS

Clinical Features

Sixty-three cases of GCTs in patients 18 years of age and below were identified. Cases occurred in 20 male (32%) and 43 female (68%) patients ranging in age from 8 to 18 years (median, 16 y). Anatomic sites included the tibia (n = 16, 25%), the femur (n = 14, 22%), the vertebral body (n = 13, 21%), the radius (n = 4; 6%), the humerus (n = 4, 6%), the metacarpal bone (n = 3, 5%), the fibula (n = 2, 3%), the patella (n = 2, 3%), and 1 each (2%) in the calcaneus, navicular, phalanx, pelvis, and ulna. One patient, a 13-year-old boy, had multifocal disease with involvement of the second metacarpal bone and distal radius. None of the patients had clinical features of hyperparathyroidism.

Radiologic Findings

Radiologic images (n = 15) or reports (n = 37) were available for review in 52 cases. Available imaging studies included conventional radiographs (n = 13), computed tomographic (n = 4), and magnetic resonance imaging (n = 2). All 15 cases with radiologic images demonstrated an osteolytic pattern of destruction, with 14 of the 15 showing variable degrees of expansion of the bone (Fig. 1). The majority of the lytic lesions had a narrow zone of transition (12/15 cases, 80%), with only 2 of the 15 showing a peripheral rim of sclerosis (13%). Two of 15 lesions were associated with a pathologic fracture (13%). Evaluation of skeletal maturity revealed 7 patients with open physes (47%) and 8 patients with closed growth plates (53%).

For the 37 cases with radiologic reports only, all reports described an osteolytic pattern of destruction,

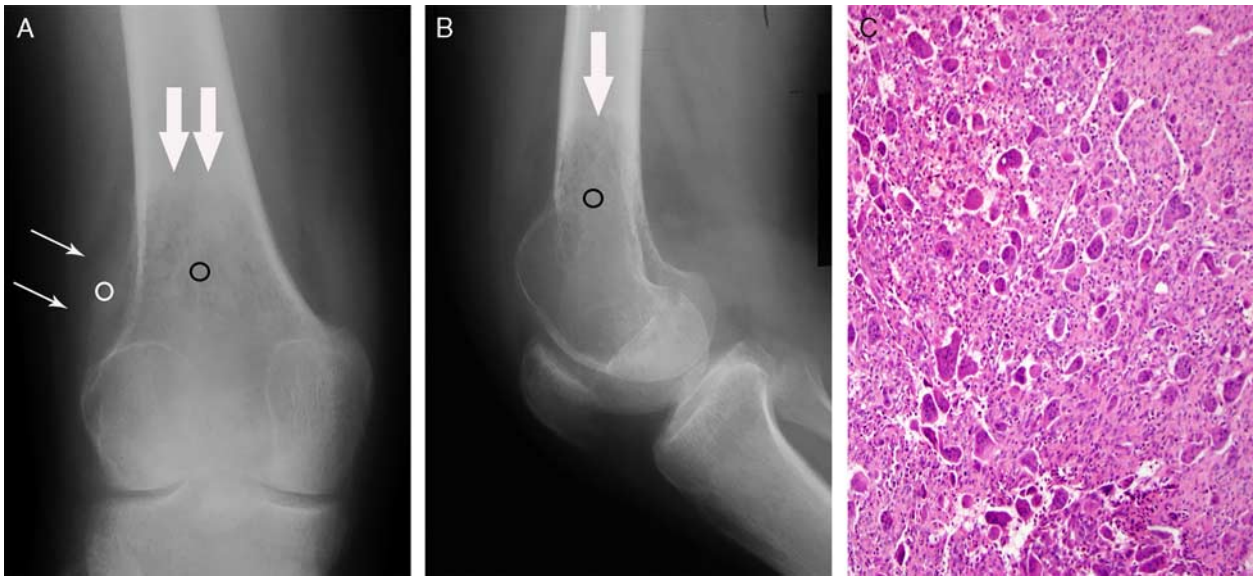

FIGURE 2. Anteroposterior (A) and lateral (B) radiographs of the knee of a skeletally mature 18-year-old boy show a partially expansile osteolytic lesion in the distal femoral metadiaphysis that extends to involve a portion of the epiphysis. The lesion has a relatively narrow zone of transition (thick arrows) but has a permeative pattern of destruction in the cortex posterolaterally (black circle). There is aggressive periosteal new bone formation along with an associated soft tissue mass laterally that contains osteoid-type matrix (white circle). The radiographic differential diagnosis includes aneurysmal bone cyst, GCT (possibly with secondary aneurysmal bone cyst), and osteosarcoma. (C) Microscopic examination showed classic features of GCT (hematoxylin and eosin stain).

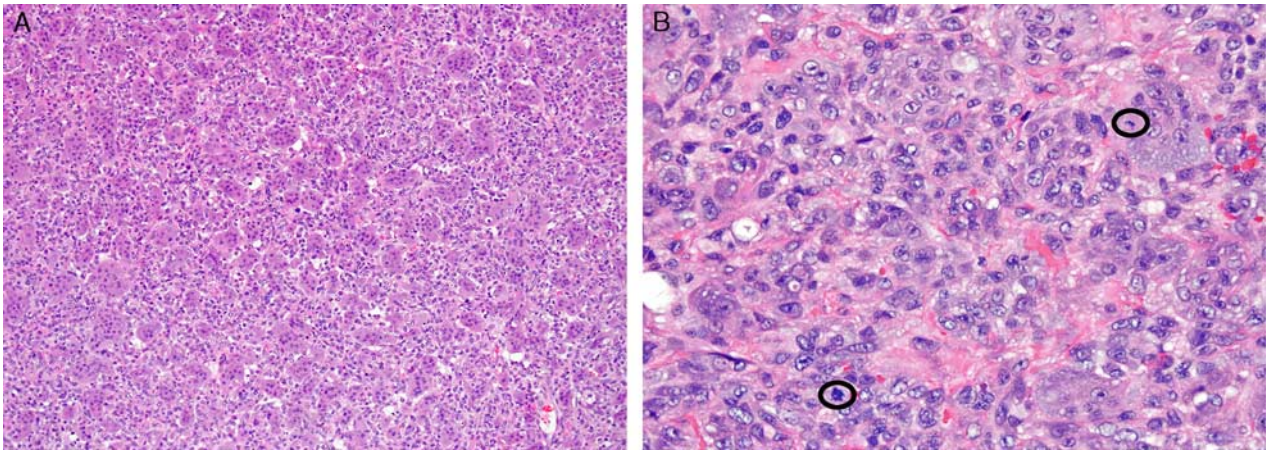

FIGURE 3. Microscopically all tumors showed classic histologic features of GCT, including evenly spaced multinucleated osteoclast-like giant cells in a background of uniform mononuclear cells (A). Mitotic rates of these tumors were variable (circle), but atypical mitoses were absent (B) (A and B: hematoxylin and eosin stain).

with 19 cases exhibiting associated osseous expansion (51%). Pathologic fracture was noted in 7 cases in this subset (19%). There was no information regarding skeletal maturity for this cohort.

Radiologic data were available for 33 of the 47 tumors that involved bones with an epiphysis or epiphyseal equivalent (Table 1). Seven (21%) cases involved the metaphysis without extension into the epiphysis (ages, 9 to 16 y; median, 13 y), whereas 23 (70%) cases involved the epiphysis and metaphysis (ages, 8 to 18 y; median, 17 y). In 5 of 23 (22%) cases where the tumor involved the metaphysis and epiphysis, epiphyseal involvement was minimal. Finally, 3 (9%) cases were confined to the epiphysis (ages, 13 to 18 y; median, 18 y). These groups were too small for statistical analysis. However, when comparing the age of patients and epiphyseal involvement, the median age of patients with and without epiphyseal involvement was 17 years (n = 26) and 13 years (n = 7), respectively, which was statistically significant ($P = 0.0014$).

In our series, 1 GCT in the distal femoral metadiaphysis of an 18-year-old boy showed a lytic lesion with a permeative pattern of cortical destruction and associated osteoid-containing soft tissue mass (Figs. 2A, B). Imaging also showed aggressive patterns of periosteal new bone formation in the region of the soft tissue mass with multilamellated and spiculated patterns raising suspicion for osteosarcoma. The patient underwent excision of the mass, which showed conventional GCT morphology (Fig. 8C), and he is currently alive without evidence of disease or metastasis 28 years after diagnosis.

Pathologic Features

Microscopically, all tumors showed at least focal areas with features of classic GCT, including evenly spaced multinucleated osteoclast-like giant cells in a background of mononuclear cells (Fig. 3A). The mononuclear cells had round to oval or, occasionally, spindle-shaped nuclei with vesicular chromatin, inconspicuous nucleoli, amphophilic cytoplasm, and indistinct cell borders. While the mitotic rates of these tumors varied (0 to 35 mitoses per 10 HPF; median, 5 mitoses per 10 HPF) (Fig. 3B), atypical mitoses were not identified. In addition, no tumor harbored significant cytologic atypia, and no definitive lymphovascular space invasion was appreciated.

The most common alternate morphology was fibrosis, identified in 31 cases (49%). Regional variations in the amount and type of fibrosis led to subclassification in 6 patterns. "Loose" was the most frequently encountered pattern of fibrosis noted in 11 cases (17%) and consisted of sparsely deposited bland fibroblasts and myofibroblasts in a highly vascularized hyalinized stroma (Fig. 4A). The second most common pattern termed "pericellular" fibrosis contained thin strands of fibrous tissue encasing cords, strips, and individual tumor cells (Fig. 4B). Pericellular fibrosis was found in 9 cases (14%). The "septal" and "geographic" patterns of fibrosis were each identified in 8 cases (13%), the former showing broad hypocellular bands of collagen partitioning the tumor stroma (Fig. 4C), whereas the geographic pattern showed a serpiginous arrangement of fibrosis isolating islands of conventional GCT (Fig. 4D). Paucicelluar eosinophilic zones, termed "hyalinized" fibrosis, were seen in 5 cases (8%) (Fig. 4E). The least frequently identified pattern showed irregular "lace-like" fibrosis in a haphazard arrangement (Fig. 4F) and was seen in 4 cases (6%). Although the majority of cases (21, 68%) contained a single fibrosis pattern, 10 cases exhibited 2 or more, with 1 case showing 4 patterns.

Reactive-appearing bone formation was identified in 26 (41%) cases, characterized by irregular trabeculae lined by a single layer of plump cytologically bland osteoblasts and surrounded by a loose arrangement of uniform ovoid to spindled mononuclear cells in a hypervascular stroma (Fig. 5A). Although the broad sheets of lace-like osteoid characteristic of high-grade osteosarco-

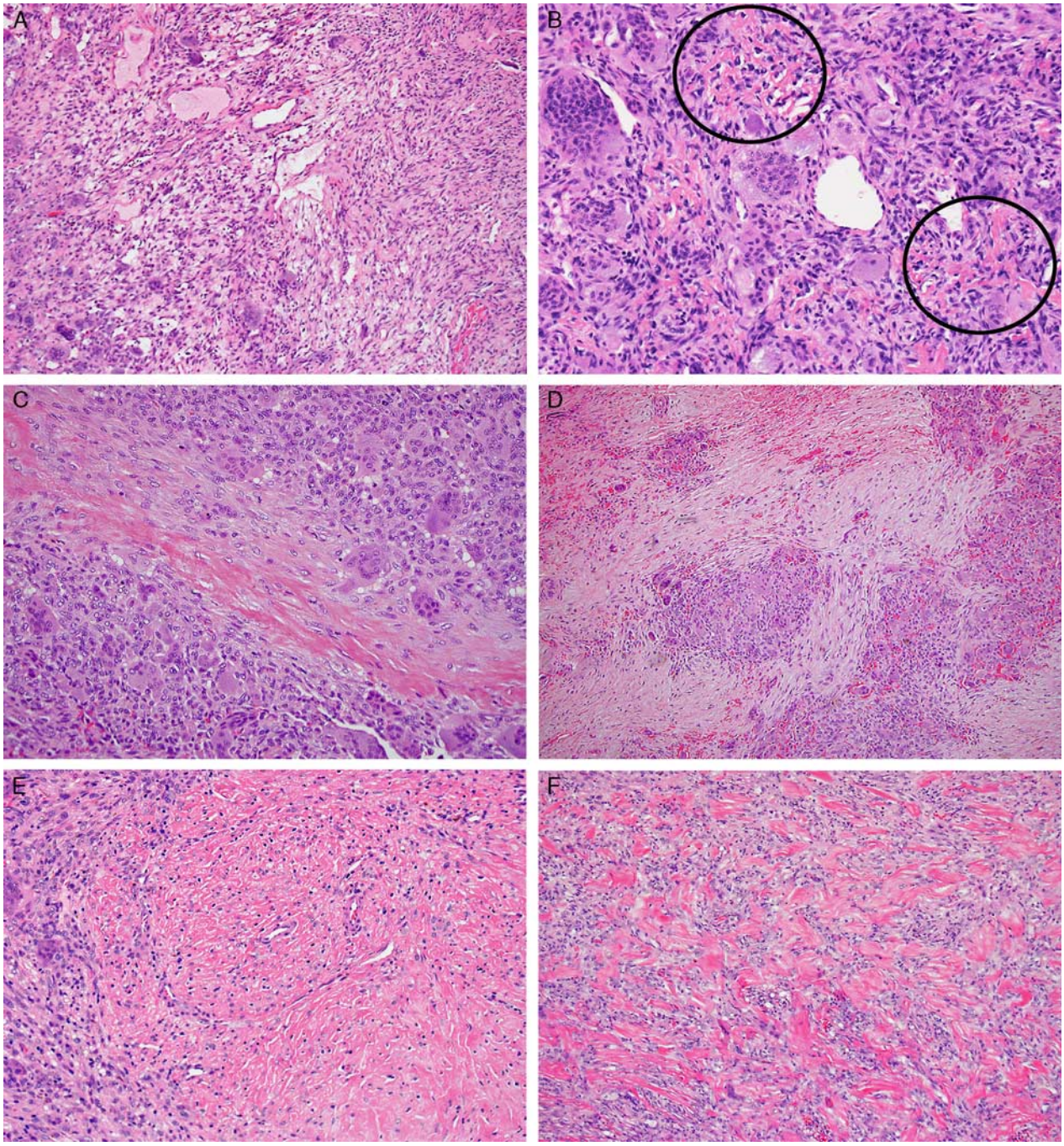

FIGURE 4. Diverse patterns of fibrosis were noted (A–F). "Loose" fibrosis (A) consisted of sparsely deposited fibroblasts and myofibroblasts in a vascular stroma. "Pericellular" fibrosis (B) contained thin strands of fibrous tissue surrounding individual tumor cells (circle). "Septal" fibrosis (C) was composed of broad bands of collagen. "Geographic" fibrosis (D) showed a serpiginous pattern of fibrosis encasing zones of conventional GCT. "Hyalinized" pattern (E) contained paucicelluar eosinophilic foci. Irregular "lace-like" fibrosis (F) showed a haphazard arrangement of dense eosinophilic collagen (A–F: hematoxylin and eosin stain).

ma were not appreciated in these tumors, a subset of cases did exhibit small foci of wispy immature osteoid deposition (Fig. 5B).

Cystic changes were identified in 7 (11%) GCTs, composed of pools of hemorrhage within the tumor (Fig. 6A). As many of these cases were curettage specimens, we only considered cases to harbor cystic change if the foci of hemorrhage were present within intact stroma. The interface between lesional cells and hemorrhage contained characteristic GCT morphology without fibrosis or seams of osteoid/bone. Two of these cases and 1 additional case showed histologic features classic for

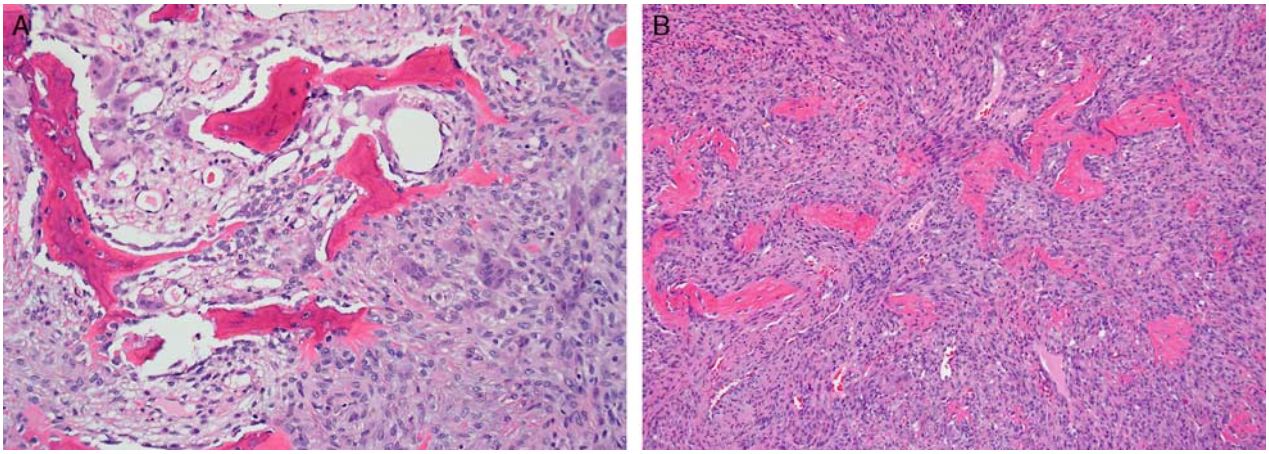

FIGURE 5. Reactive-appearing bone formation, characterized by irregular woven bony trabeculae (A) lined by a single layer of plump osteoblasts without cytologic atypia or nuclear hyperchromasia. Occasionally, the trabeculae were less developed, creating a "lace-like" osteoid pattern (B) (A and B: hematoxylin and eosin stain).

secondary aneurysmal bone cyst formation (Fig. 6B), including pools of blood surrounded by fibrous septa containing reactive-appearing (myo) fibroblasts, giant cells, and osteoid/bone.

Collections of foamy histiocytes were present in 6 (10%) cases (Figs. 6C, D), whereas 2 (3%) cases had microscopic nodules of hyaline cartilage embedded within the tumor (Fig. 6E). The foci of cartilage exhibited small clusters of chondrocytes relatively evenly distributed throughout the nodules and appeared to be a part of the tumor rather than inadvertently sampled articular cartilage.

Infarct-like necrosis was present in 17 (27%) cases and was characterized by ghost outlines of mononuclear cells and multinucleated giant cells lacking an inflammatory response (Fig. 6F). There was generally an abrupt transition between viable tumor and zones of necrosis.

All cases contained areas with conventional GCT morphology, but only 17 (27%) tumors were composed solely of "conventional histology." The alternate morphologic patterns, when identified, were typically focal and involved $<10\%$ of lesional tissue.

Molecular Genetics

Mutation analysis was performed on 5 cases of GCT, and all (5/5) had mutation in *H3F3A* (Table 2, Fig. 7). No mutations in *H3F3B* were identified.

Treatment

Treatment information was available for 55 patients. Twenty-eight patients were treated with intralesional surgery, whereas 27 patients underwent a wide resection. Two patients who underwent curettage and bone grafting also received postoperative radiation to control local disease. One patient received chemotherapy after developing lung metastases 20 months after diagnosis (see Outcomes section below).

Outcomes

Follow-up information was available for 55 patients with a range of 6 months to 69.6 years (median, 11.6 y). Twenty-one patients had local recurrence (38%), and 2 patients (4%) developed pulmonary metastases 15 and 20 months after initial diagnosis, respectively. Ten of 27 patients who underwent wide resection and 11 of 28 patients who had intralesional treatment had a local recurrence at mean follow-up of 170 months. The mean time to local recurrence was 54 months.

The 5-year progression-free survival estimate was 57% (95% confidence interval, 43%-71%). At the time of last follow-up, 51 patients were alive without evidence of disease, 1 was alive with disease, and 3 patients had died (1 had died of disease and 2 had died of other causes). The patient who had died of disease was a 16-year-old girl with GCT arising in the sacrum. She had undergone lumbosacral laminectomy with tumor debulking but subsequently developed bilateral pulmonary metastases 20 months after initial diagnosis, for which she received chemotherapy. Approximately 40 months later, she had tumor progression in the sacral region and underwent re-resection. She ultimately died of progressive local disease 66 months after initial diagnosis.

Correlation of Morphologic Features, Clinical Characteristics, and Outcome

No statistically significant correlation was found between morphologic patterns (reactive-appearing bone, fibrosis, cystic change, secondary aneurysmal bone cysts, foamy histiocytes, cartilage) and anatomic site, sex, patient age, or outcome. When comparing site and outcome, we noted that the 5-year progression-free survival of tumors occurring in the long tubular bones, vertebral bodies, and all remaining sites was 68%, 50%, and 25%, respectively (Table 3). Specifically comparing tumors arising in the long tubular bones versus those arising at all other sites excluding the vertebral bodies, we found that the former had a statistically significantly

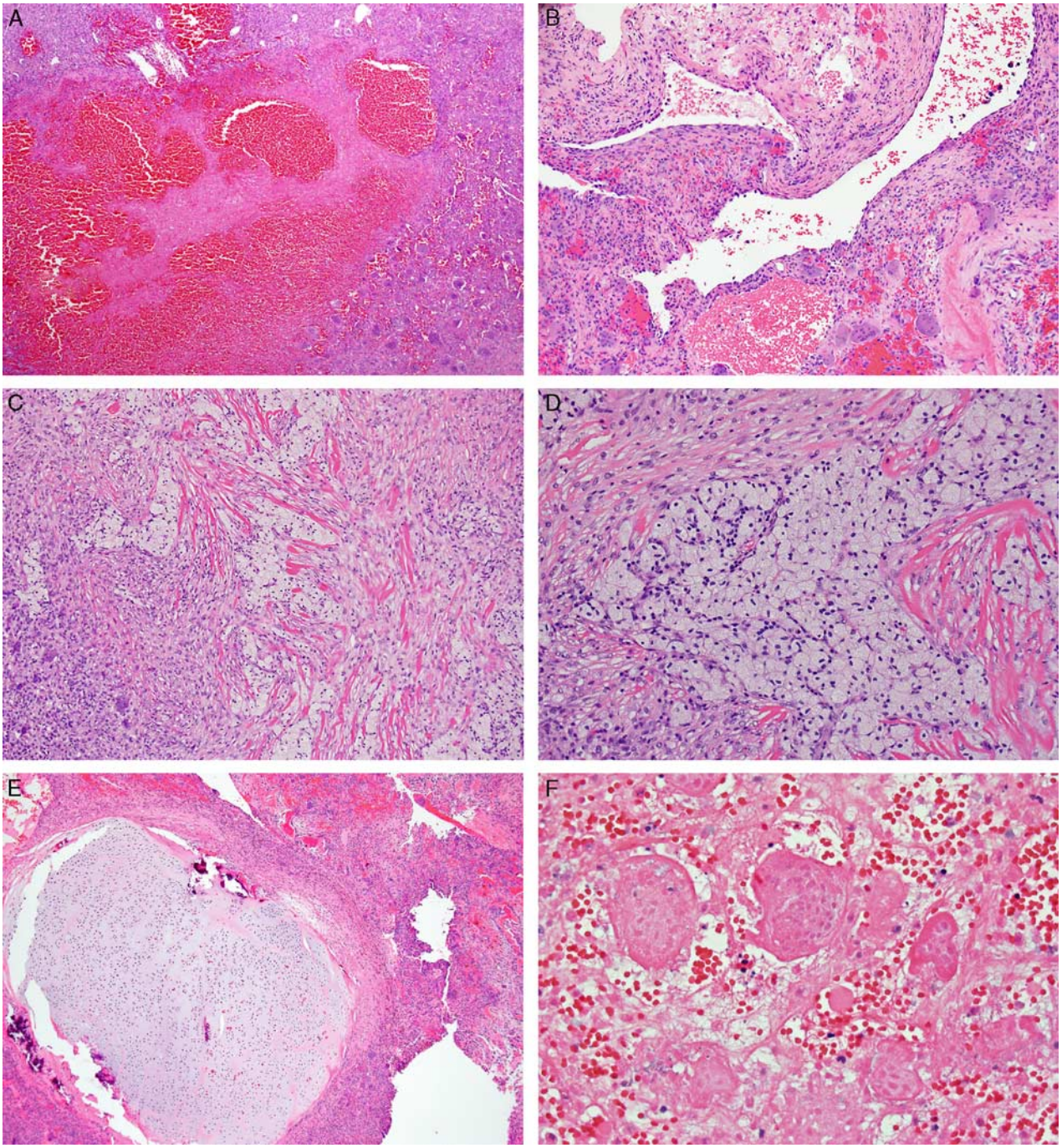

FIGURE 6. Other morphologic patterns included cystic changes (A), secondary aneurysmal bone cyst formation (B), collections of foamy histiocytes (shown at low [C] and high [D] magnification) (C and D), microscopic nodule of hyaline cartilage embedded within the GCT (E), and infarct-like necrosis (F) (A–F: hematoxylin and eosin stain).

lower risk for adverse events (recurrences/metastasis). The presence of infarct-like necrosis, pathologic fracture, patient age, and mitotic rate failed to correlate significantly with progression-free survival even though there was a trend toward increased recurrence and metastasis with increased mitotic rate (Fig. 8) ($P = 0.18$ when considered categorically, $P = 0.06$ when considered continuously with hazard ratio of 1.06) (Table 3). Finally, when assessing reactive-bone formation and infarct-like necrosis, there was no significant association between these features and the presence of fracture ($P = 0.72$ and 1.0, respectively).

TABLE 2. Selected Cases for *H3F3A* and *H3F3B* Mutation Analysis

Case	Age/Sex	Site	E/M/D	*H3F3A* Status	*H3F3B* Status
1	16/Female	Femur	E, M, D	G34W (GGG > TGG)	WT
2	17/Male	Fibula	E, M	G34L (GGG > TTG)	WT
3	15/Female	Humerus	M, D	G34W (GGG > TGG)	WT
4	13/Male	Tibia	M, D	G34W (GGG > TGG)	WT
5	13/Male	Metacarpal	M, D	G34W (GGG > TGG)	WT

D indicates diaphysis; E, epiphysis; M, metaphysis; WT, wild type.

DISCUSSION

GCT of the bone is a rare neoplasm with a characteristic clinical, radiologic, and morphologic appearance. The vast majority of these tumors occur in skeletally mature adults between the ages of 20 and 60 years, with a female predominance.[3] In fact, the pathologist is typically cautioned to consider the diagnosis of GCT in patients younger than 20 years with skepticism.[25,26] Although the occurrence of GCT in the pediatric population (patients 18 y old or younger) has been well documented (Table 4), these studies focus primarily on radiologic features, with the remaining reports combining the histologic features of adults and pediatric age groups together. Variable amounts of bone formation and fibrosis can be seen in GCT. When these features are present in pediatric patients, diagnoses more common in this age group, such as aneurysmal bone cyst, chondroblastoma, and, most importantly, osteosarcoma, are considered. Therefore, we sought to examine a large series of pediatric GCTs to fully characterize the morphologic spectrum of this entity.

Our data demonstrate that GCTs in patients 18 years or younger accounted for 9% of all GCTs seen at our institution over the last 100 years. This incidence falls within the range reported in the literature (range, 1.7% to 10.6%).[12,15,17,19] The female to male distribution in our study was approximately 2:1, concordant with the strong female predominance that has been a consistent observation of GCT in the pediatric population.[12,17] The most common anatomic location in our series of GCT was the tibia (25%), followed by the femur (22%) and then the vertebral body (21%), similar to what has been reported in other pediatric studies.[15,17]

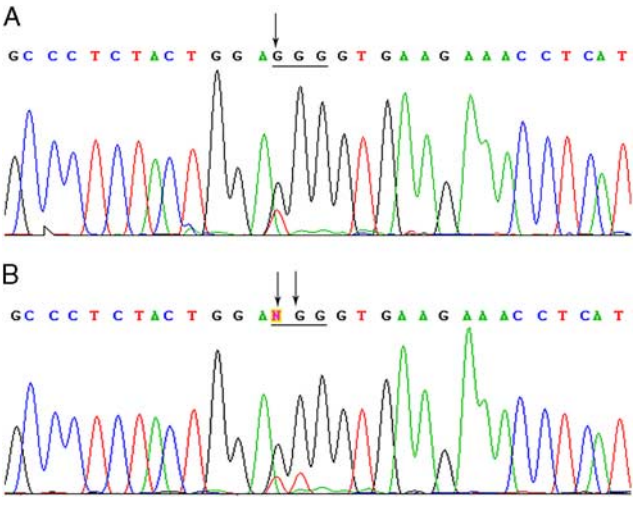

FIGURE 7. *H3F3*A mutation analysis by polymerase chain reaction and Sanger sequencing. A, GCT with G34W (GGG > TGG). B, GCT with G34L (GGG > TTG). Arrows indicate the location of point mutations.

Although the imaging characteristics of the GCTs in this study were compatible with those found in adult patients, including an expansile and eccentric lytic lesion with a narrow zone of transition, we did note that 21% of tumors arising in a bone with an epiphysis or epiphyseal equivalent lacked epiphyseal involvement. This contrasts with adult GCTs that almost universally involve the epiphysis.[2,3] Prior studies have also noted that purely metaphyseal or metadiaphyseal lesions are more common in children,[2,3] suggesting that GCT originates from the metaphysis.[12] In our series the median age of patients without epiphyseal involvement was 13 years compared with 17 years for patients with epiphyseal involvement, which was statistically significant, supporting this theory.

Histologically, all cases in this series contained areas of conventional GCT, including evenly spaced multinucleated cells in a background of cytologically bland round to oval or, occasionally, spindle-shaped mononuclear cells. However, only approximately one fourth of cases consisted solely of this classic morphology. Alternate morphologies, which were typically focal, included fibrosis (49%), reactive-appearing bone (41%), cystic change (11%), foamy histiocytes (10%), secondary aneurysmal bone cyst (5%), and hyaline cartilage (3%).

Nearly half of the GCTs in this study contained foci of fibrosis. The regional variations of fibrosis that our cases harbored were quite diverse, including loose, pericellular, hyalinized, geographic, septal, and lace-like patterns. Importantly, in areas with fibrosis, giant cells may be sparse, unevenly spaced, or entirely absent, leading to the consideration of other entities such as solid aneurysmal bone cyst, nonossifying fibroma, or Brown tumor of hyperparathyroidism. If the entire lesion is available for review, identifying areas with conventional GCT will aid in the correct diagnosis. However, classification may be more difficult on a biopsy specimen, and in this scenario correlation with clinical, radiologic, and at times molecular findings is essential. Clinical evaluation of calcium, phosphorus, and parathyroid hormone levels is imperative when one considers the diagnosis of Brown tumor of primary hyperparathyroidism.[27,28] Anatomic

TABLE 3. Progression-free Survival Estimates Among Patients With Follow-up

Variables	N	No. Adverse Events	95% CI 5-Year Progression-free Survival (%)	Hazard Ratio	*P*
Site					0.04
Long tubular bone	34	10	67.7% (51.0%-84.3%)	Reference	
Vertebral body	12	6	50.0% (21.7%-78.3%)	2.12 (0.72-5.72)	
All others	9	6	25.4% (0.0%-55.7%)	3.78 (1.27-10.31)	
Infarct-like necrosis					0.85
Absent	40	16	57.4% (41.4%-73.5%)	Reference	
Present	15	6	55.6% (28.8%-82.3%)	0.91 (0.33-2.22)	
Pathologic fracture					0.69
Absent	40	16	57.0% (40.9%-73.1%)	Reference	
Present	9	3	66.7% (35.9%-97.5%)	0.79 (0.18-2.36)	
Age (y)					0.26
≤13	8	5	37.5% (4.0%-71.0%)	Reference	
14-16	18	6	66.2% (44.1%-88.3%)	0.36 (0.11-1.25)	
≥17	29	11	55.9% (35.8%76.0%)	0.48 (0.17-1.52)	
Mitoses per 10 HPF					0.18
≤3/10 HPF	18	5	71.1% (49.7%-92.5%)	Reference	
4-8	19	7	55.4% (29.5%81.2%)	1.84 (0.58-6.22)	
≥9	18	10	43.8% (20.5%-67.0%)	2.67 (0.94-8.59)	
Continuous (HR for 1-level increase)				1.06 (1.00-1.11)	0.06

Adverse events indicates recurrence or metastasis; CI, confidence interval.

location may also provide important clues. Giant cell reparative granulomas arise in the jaw, whereas GCT rarely involves craniofacial bones.[29,30] When confronted with the differential diagnosis of solid aneurysmal bone cyst versus GCT, particularly when the tumor is centered in the metaphysis, evaluation for *USP6* rearrangement may be a helpful ancillary study, as approximately 70% of aneurysmal bone cysts will harbor this genetic aberration.[31–33] FISH studies for *USP6* also may be useful in tumors exhibiting cystic changes leading to consideration of primary conventional aneurysmal bone cyst.

The next most common morphologic pattern identified in our series was reactive-appearing bone. In a study by Goldenberg et al,[5] approximately 35% of GCTs showed osteoid or bone formation. Similarly, we found bone formation in approximately 40% of cases, appearing predominantly reactive in nature with plump osteoblasts rimming irregular bone trabeculae. Occasionally, the trabeculae appeared immature, creating a "lace-like" osteoid pattern. The pathogenesis of bone formation within these tumors remains unclear. The bone in our cases appeared to be embedded within the tumor, unlike the peripheral rim of woven bone characteristically seen at the advancing margin of GCT. Although we hypothesized that this feature may correlate with the presence of a pathologic fracture, age, or anatomic site, we did not find significant correlation.

The presence of bone, especially when immature, may raise concern for giant cell–rich osteosarcoma, particularly in metaphyseal lesions, the most common site for

TABLE 4. Previously Reported Case Series of Pediatric GCT

References	No. Cases	Age (s) (y)	Male/Female	Outcome
Sherman and Fabricius[6]	1	15	1/0	LR
Mnaymneh et al[4]	12	12-19	NA	8% LR
Johnson and Riley[7]	3	10-19	0/3	33% LR
Goldenberg et al[5]	38	13-19	11/27	NA
Larsson et al[8]	2	16-18	2/0	NLR
Larsson et al[9]	12	4-19	9/3	NA
Peison and Feigenbaum[10]	1	14	0/1	LR
Minguella[11]	1	6	0/1	NLR
Picci et al[12]	6	10-14	1/5	NLR
Kaufman et al[13]	1	13	1/0	NA
Dahlin[3]	65	< 20	18/47	NA
Mcdonald et al[14]	45	10-20	11/34	NA
Campanacci et al[2]	10	10-20	NA	NA
Kransdorf et al[15]	50	1.5-18	29/21	NA
Fain et al[16]	7	8-18	5/2	NLR
Schutte and Taconis[17]	49	4-18	18/31	8% LR
Krajca-Radcliffe et al[18]	2	2-3	0/2	NLR
Puri et al[19]	17	10-18	3/14	20% LR

LR indicates local recurrence; NA, not available; NLR, no local recurrence.

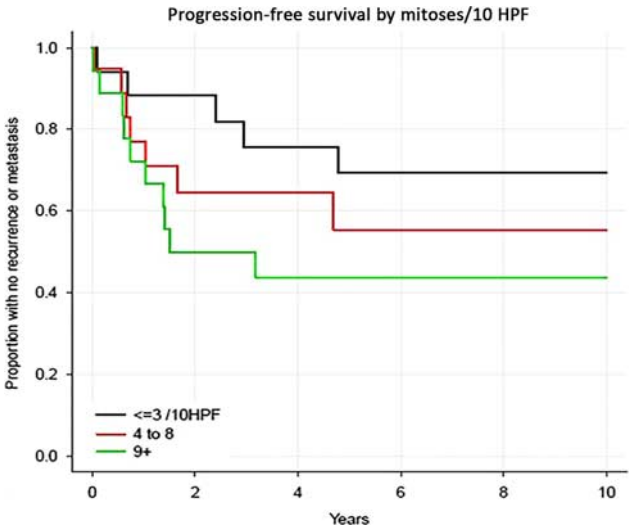

FIGURE 8. Mitotic rate failed to correlate significantly with progression-free survival even though there was a trend toward increased recurrence and metastasis with increased mitotic rate.

intramedullary osteosarcoma. Correlation with imaging is typically helpful as most GCTs present as a well-defined, eccentric lytic lucency.[4,14,34] However, the radiologic features of GCT may appear aggressive, adding to concern for malignancy. For example, 1 GCT in our series showed aggressive imaging features. In such cases with worrisome radiologic findings, a preoperative image-guided needle biopsy is usually obtained, making histologic analysis particularly difficult because of a limited amount of tissue. In this situation, it is even more critical for pathologists to be aware of the histologic spectrum of GCT.

In tumors with bone formation eliciting a differential diagnosis including GCT and osteosarcoma, careful review of the cytologic features of the tumor cell population is critical. The monoclear cells of classic GCT should be uniform, mirroring the nuclei within the giant cells. However, areas composed of bland spindle-shaped cells are not uncommon. The neoplastic cells of high-grade osteosarcoma will show significant pleomorphism and hyperchromatism, features not permissible for a diagnosis of GCT. Mitotic figures are not a useful discriminatory finding, as mitotic figures are often readily identifiable in GCT.[35,36] The presence of atypical mitoses, however, supports a diagnosis of malignancy.

Two cases had microscopic nodules of hyaline cartilage embedded within the tumor. The presence of cartilage in an epiphyseal mass in a pediatric patient may raise the possibility of chondroblastoma. However, the chondroid matrix in chondroblastoma is pink, occasionally containing pale blue areas, as opposed to the homogenous blue color of the hyaline cartilage. The mononuclear cells of chondroblastoma, often admixed with scattered multinucleated giant cells, can also resemble those of a GCT. The distinction can be made by paying close attention to the cytologic features. In contrast to GCT, chondroblastoma contains elongated nuclei with longitudinal grooves and rather well-defined cytoplasmic borders. From a radiologic standpoint, chondroblastomas present as lytic lesions in the epiphysis with a well-defined peripheral rim of sclerosis in contrast to GCT, which involves the epiphysis but frequently extends to the metaphysis and show a lytic pattern of destruction with a narrow zone of transition with a peripheral rim of sclerosis. Furthermore, magnetic resonance images of chondroblastoma show prominent peritumoral edema.

A small subset of our GCTs harbored foamy histiocytes, and 80% (4/5 cases) of these also showed foci of fibrosis. The combination of fibrosis and foamy histiocytes may mimic nonossifying fibroma (metaphyseal fibrous defect), a lesion that classically presents in childhood and usually contains multinucleated giant cells. Fortunately, nonossifying fibroma has a characteristic appearance on imaging, including an eccentric cortically based lytic lesion with scalloped and sclerotic margins arising in the metaphysis and metadiaphysis. Histologically, it lacks the classic mononuclear cells of GCT, and the entire tumor is composed of spindle-shaped cells arranged in a storiform pattern.

GCT may be locally aggressive with recurrence rates ranging from 15% to 50%, and pulmonary metastases occur in approximately 2% of cases of GCT with conventional morphology.[37] Schutte and Taconis[17] demonstrated a lower recurrence rate in children than in adults, whereas in a study performed by Puri et al [19] the recurrence rate was similar to that of the adult population. Twenty-one (31%) patients in our study had local recurrence, whereas pulmonary metastases were reported in 2 (4%), concordant with previously reported data. Although tumors arising in long tubular bones had a better 5-year progression-free survival compared with tumors arising at all other sites exclusive of vertebral bodies, we were unable to find any significant correlation between morphologic patterns, infarct-like necrosis, pathologic fracture, or mitotic rate and outcome.

Finally, we were able to perform mutation analysis on 5 cases in our series, 3 of which lacked epiphyseal involvement. The identification of *H3F3A* mutations in these tumors supports the diagnosis of GCT and provides further evidence that GCT may spare the epiphysis.

In summary, the morphologic spectrum of GCT in pediatric patients is broad, and the majority of tumors harbor at least 1 histologic feature that differs from the classical GCT morphology. Even though these alternate morphologic patterns are similar to what can be seen in adult GCT and do not appear to correlate with outcome, it is important for pathologists to recognize that these features may be present to prevent misclassification as other giant cell–rich lesions seen in childhood. Importantly, findings such as bone formation, fibrosis, and increased mitoses are common in GCT in this age group and should not lead to a misdiagnosis of osteosarcoma, a tumor more commonly seen in the pediatric population. Careful review of cytologic features, correlation with

radiologic findings, and use of molecular studies, when appropriate, are essential for accurate diagnosis.

REFERENCES

1. Unni KK, Inwards CY. *Dahlin's Bone Tumors: General Aspects and Data on 11087 Cases*. Philadelphia, PA: Lippincott Williams & Williams; 2010:179–183. 310-316.
2. Campanacci M, Baldini N, Boriani S, et al. Giant-cell tumor of bone. *J Bone Joint Surg Am*. 1987;69:106–114.
3. Dahlin DC. Caldwell lecture. Giant cell tumor of bone: highlights of 407 cases. *AJR Am J Roentgenol*. 1985;144:955–960.
4. Mnaymneh WA, Dudley HR, Mnaymneh LG. Giant-cell tumor of bone. An analysis and follow-up study of the forty-one cases observed at the Massachusetts General Hospital between 1925 and 1960. *J Bone Joint Surg Am*. 1964;46:63–75.
5. Goldenberg RR, Campbell CJ, Bonfiglio M. Giant-cell tumor of bone. An analysis of two hundred and eighteen cases. *J Bone Joint Surg Am*. 1970;52:619–664.
6. Sherman M, Fabricius R. Giant-cell tumor in the metaphysis in a child. Report of an unusual case. *J Bone Joint Surg Am*. 1961;43-A:1225–1229.
7. Johnson KA, Riley LH Jr. Giant cell tumor of bone. An evaluation of 24 cases treated at the Johns Hopkins Hospital between 1925 and 1955. *Clin Orthop Relat Res*. 1969;62:187–191.
8. Larsson SE, Lorentzon R, Boquist L. Giant-cell tumors of the spine and sacrum causing neurological symptoms. *Clin Orthop Relat Res*. 1975;111:201–211.
9. Larsson SE, Lorentzon R, Boquist L. Giant-cell tumor of bone. A demographic, clinical, and histopathological study of all cases recorded in the Swedish Cancer Registry for the years 1958 through 1968. *J Bone Joint Surg Am*. 1975;57:167–173.
10. Peison B, Feigenbaum J. Metaphyseal giant-cell tumor in a girl of 14. *Radiology*. 1976;118:145–146.
11. Minguella J. Giant cell tumour of metacarpal in a child of unusual site and age. *Hand*. 1982;14:93–96.
12. Picci P, Manfrini M, Zucchi V, et al. Giant-cell tumor of bone in skeletally immature patients. *J Bone Joint Surg Am*. 1983;65:486–490.
13. Kaufman RA, Wakely PE, Greenfield DJ. Case report 224. Giant cell tumor of ossification center of the distal end of the fibula, growing into the metaphysis. *Skeletal Radiol*. 1983;9:218–222.
14. McDonald DJ, Sim FH, Mcleod RA, et al. Giant-cell tumor of bone. *J Bone Joint Surg Am*. 1986;68:235–242.
15. Kransdorf MJ, Sweet DE, Buetow PC, et al. Giant cell tumor in skeletally immature patients. *Radiology*. 1992;184:233–237.
16. Fain JS, Unni KK, Beabout JW, et al. Nonepiphyseal giant cell tumor of the long bones. Clinical, radiologic, and pathologic study. *Cancer*. 1993;71:3514–3519.
17. Schutte HE, Taconis WK. Giant cell tumor in children and adolescents. *Skeletal Radiol*. 1993;22:173–176.
18. Krajca-Radcliffe JB, Thomas JR, Nicholas RW. Giant-cell tumor of bone: a rare entity in the hands of children. *J Pediatr Orthop*. 1994;14:776–780.
19. Puri A, Agarwal MG, Shah M, et al. Giant cell tumor of bone in children and adolescents. *J Pediatr Orthop*. 2007;27:635–639.
20. Behjati S, Tarpey PS, Presneau N, et al. Distinct H3F3A and H3F3B driver mutations define chondroblastoma and giant cell tumor of bone. *Nat Genet*. 2013;45:1479–1482.
21. Cleven AH, Hocker S, Briaire-de Bruijn I, et al. Mutation analysis of H3F3A and H3F3B as a diagnostic tool for giant cell tumor of bone and chondroblastoma. *Am J Surg Pathol*. 2015;39:1576–1583.
22. Kallappagoudar S, Yadav RK, Lowe BR, et al. Histone H3 mutations—a special role for H3.3 in tumorigenesis? *Chromosoma*. 2015;124:177–189.
23. Lan F, Shi Y. Histone H3.3 and cancer: a potential reader connection. *Proc Natl Acad Sci U S A*. 2015;112:6814–6819.
24. Team RCR. *A Language and Environment for Statistical C*. Vienna, Austria: R Foundation for Statistical Computing; 2014. Available at: http://R-project.org/.
25. Czerniak B. *Dorfman and Czerniak's Bone Tumors*. 2nd ed. Philadelphia, PA: Elsevier; 2015:692–736.
26. Jaffe HL. Giant-cell tumour (osteoclastoma) of bone: its pathologic delimitation and the inherent clinical implications. *Ann R Coll Surg Engl*. 1953;13:343–355.
27. Bandeira F, Cassibba S. Hyperparathyroidism and bone health. *Curr Rheumatol Rep*. 2015;17:48.
28. Phulsunga RK, Parghane RV, Kanojia RK, et al. Multiple brown tumors caused by a parathyroid adenoma mimicking metastatic bone disease from giant cell tumor. *World J Nucl Med*. 2016;15:56–58.
29. Wolfe JT III, Scheithauer BW, Dahlin DC. Giant-cell tumor of the sphenoid bone. Review of 10 cases. *J Neurosurg*. 1983;59:322–327.
30. Roy S, Joshi NP, Siqamani E, et al. Clival giant cell tumor presenting with isolated trigeminal nerve involvement. *Eur Arch Otorhinolaryngol*. 2013;270:1167–1171.
31. Agaram NP, LeLoarer FV, Zhang L, et al. USP6 gene rearrangements occur preferentially in giant cell reparative granulomas of the hands and feet but not in gnathic location. *Hum Pathol*. 2014;45:1147–1152.
32. Oliveira AM, et al. USP6 and CDH11 oncogenes identify the neoplastic cell in primary aneurysmal bone cysts and are absent in so-called secondary aneurysmal bone cysts. *Am J Pathol*. 2004;165:1773–1780.
33. Oliveira AM, Perez-Atayde AR, Inwards CY, et al. USP6 (Tre2) fusion oncogenes in aneurysmal bone cyst. *Cancer Res*. 2004;64:1920–1923.
34. Hodges FJ, Latourette HB, Macintyre RS. Radiologic aspects of giant-cell tumor of bone. *Clin Orthop*. 1956;7:82–92.
35. Present D, Bertoni F, Hudson T, et al. The correlation between the radiologic staging studies and histopathologic findings in aggressive stage 3 giant cell tumor of bone. *Cancer*. 1986;57:237–244.
36. Unni KK, Inwards CY. *AFIP Atlas of Tumor Pathology*. *Tumors of the Bone and Joints*, 4th series. Washington, DC: American Registry of Pathology and Armed Forces Institute of Pathology; 2005. Fascicle 22005.
37. Siebenrock KA, Unni KK, Rock MG. Giant-cell tumour of bone metastasising to the lungs. A long-term follow-up. *J Bone Joint Surg Br*. 1998;80:43–47.